Cancer Cell, Volume *43*

Supplemental information

Understanding and reversing mammary tumor-driven reprogramming of myelopoiesis to reduce metastatic spread

Hannah Garner, Moreno Martinovic, Ning Qing Liu, Noor A.M. Bakker, Irene Querol Velilla, Cheei-Sing Hau, Kim Vrijland, Daphne Kaldenbach, Marleen Kok, Elzo de Wit, and Karin E. de Visser

Supplemental Figure 1

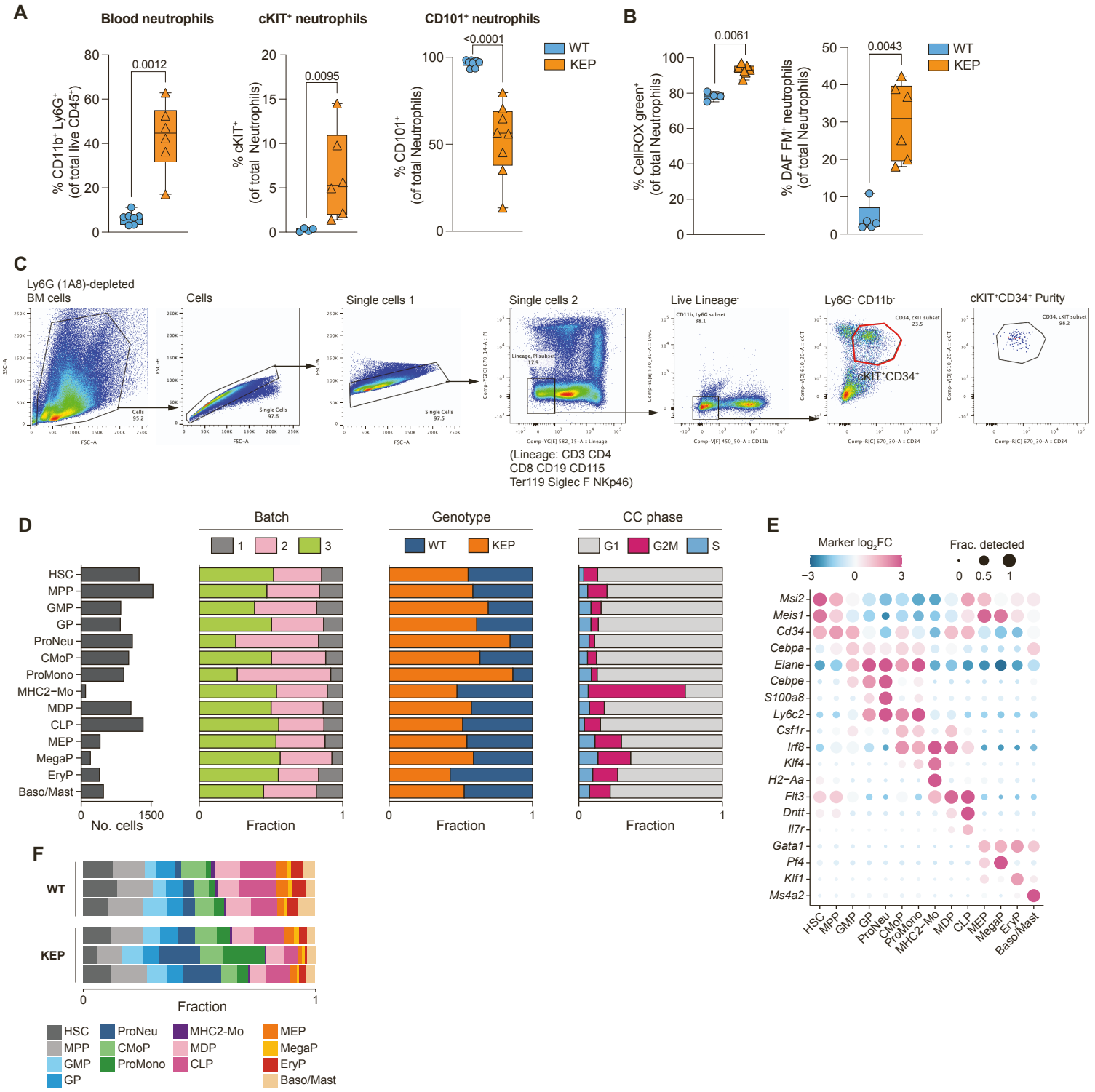

Supplemental Figures

Figure S1. Increased mouse neutrophils in tumor-bearing mice and scRNA-seq set up. Related to Figure 1

(A) Proportions of circulating total neutrophils (left), cKIT$^+$ neutrophils (middle) and CD101$^+$ neutrophils (right) from WT (blue, n=4-9) and KEP mice (orange, n=6-9).

(B) Neutrophil reactive oxygen species production as measured by *ex vivo* CellROX green flow cytometry assay (left) and neutrophil nitric oxide production as measured by DAF-FM diacetate fluorescence (right) from WT (blue, n=4-5) and KEP (orange, n=6-7) mice.

(C) Gating strategy for sorting cKIT$^+$CD34$^+$ from neutrophil (1A8)-depleted BM cells from WT (n=3) and KEP (n=3) mice. Sorted population is highlighted by red gate and representative purity plot indicated. Cells sorted across 2 independent experiments.

(D) Distributions of cell numbers, batches (each batch contains a WT-KEP littermate pair), sample genotypes and inferred cell cycle phase assignments across annotated cell types.

(E) Average log fold changes and the fractions of cells with detected marker genes used to annotate the cell types. Log fold changes were computed for each cell type compared to all other cell types.

(F) Cell number distribution across cell types and individual samples (n=3 per genotype).

Statistics: Mann-Whitney *U*-test, $p < 0.05$ considered significant. Box and whisker plots: boxes represent median and interquartile range; whiskers represent full range.

Abbreviations: HSC, hematopoietic stem cell; MPP, multipotent progenitor; GMP, granulocyte monocyte progenitor; GP, granulocyte progenitor; ProNeu, pro-neutrophils; cMoP, common monocyte progenitor; ProMono, pro-monocyte; MHC2-Mo, MHC-II$^+$ monocytes; MDP, monocyte dendritic cell progenitor; CLP, common lymphocyte progenitor; MEP, megakaryocyte erythrocyte progenitor; MegaP, megakaryocyte progenitor; EryP, erythrocyte progenitor; Baso/Mast, basophil mast cell progenitor.

Supplemental Figure 2

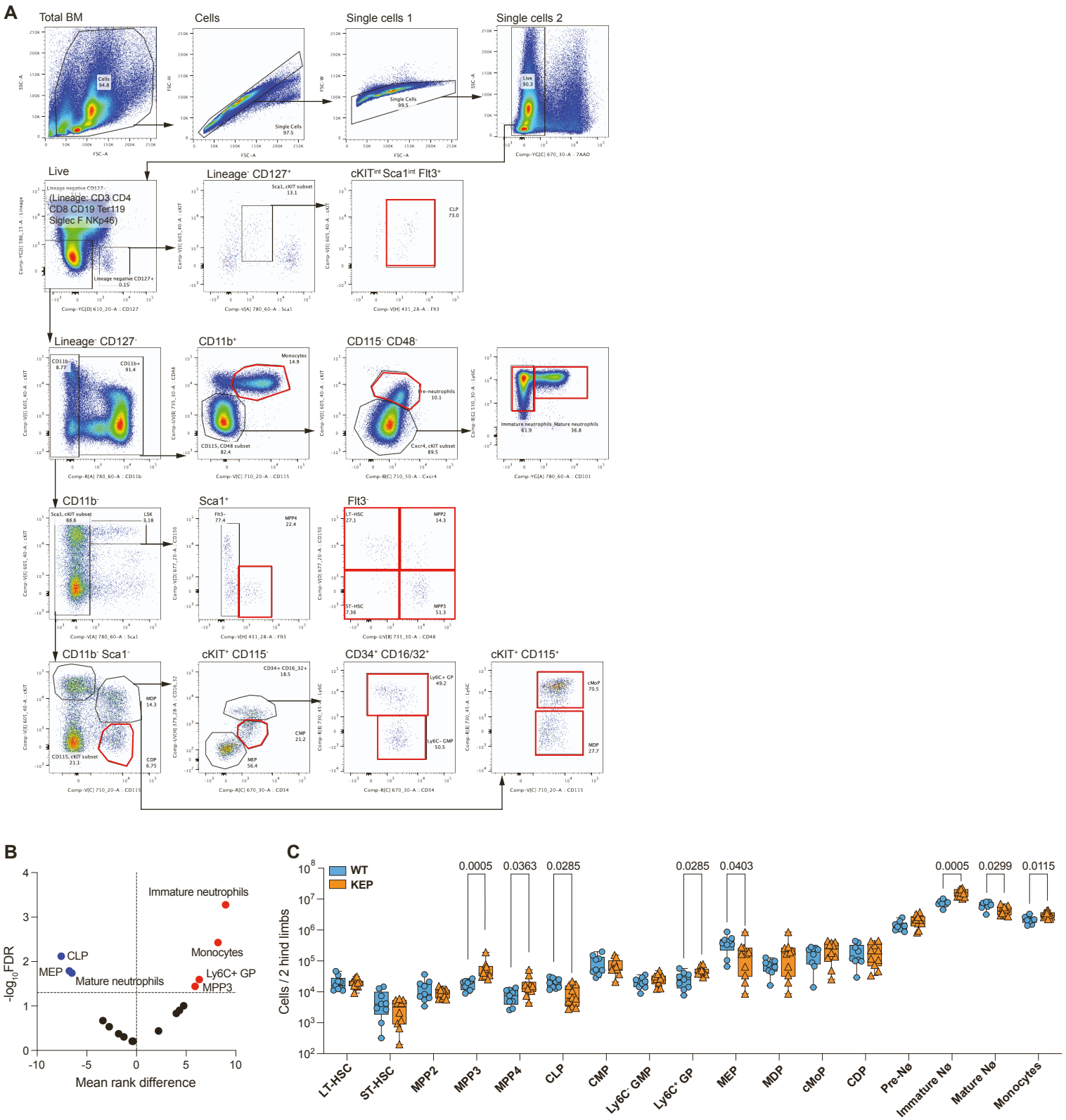

Figure S2. Flow cytometry analysis of BM populations in WT and tumor-bearing KEP mice. Related to Figure 1

(A) Gating strategy for BM populations as analyzed by flow cytometry. Reported population gates are highlighted by red gate.

(B) Volcano plot depicting difference in mean rank (as determined by Mann-Whitney *U*-test in Figure 1E) in populations from KEP mice vs. WT against adjusted p-values ($-\log_{10}$ FDR).

(C) Absolute cell counts of populations reported in Figure 1E, calculated from cell counts from 2 hindlimbs. Mann-Whitney with Benjamini, Krieger and Yekutieli's multiple comparison correction, q-value <0.05 considered significant. Data collected across 9 independent experiments. Box and whisker plots: boxes represent median and interquartile range; whiskers represent full range.

Supplemental Figure 3

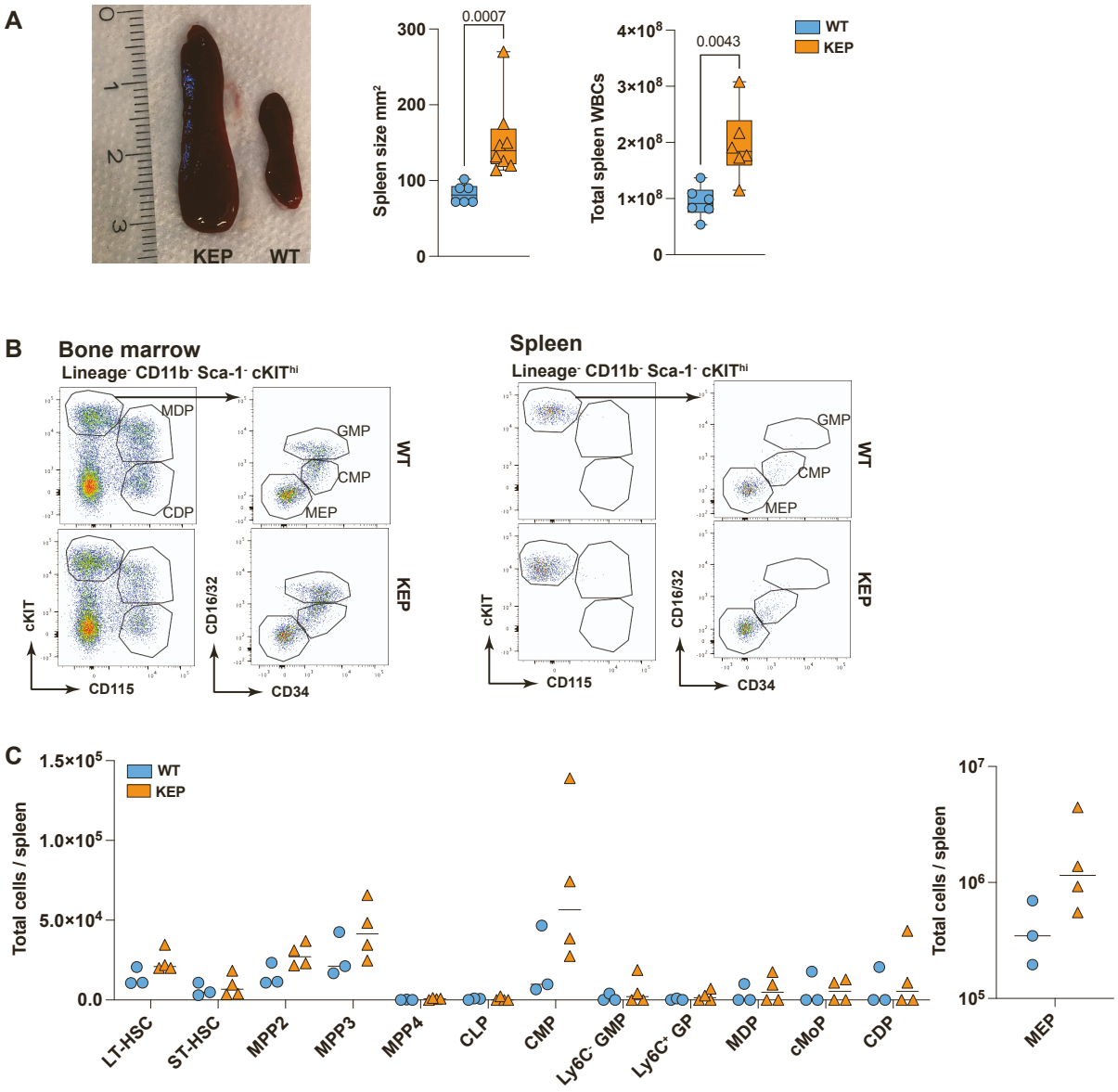

Figure S3. Spleens from tumor-bearing mice do not show evidence of early myelopoiesis. Related to Figure 1.

(A) Representative photo showing spleen size in KEP and WT mice (right), quantification of splenic area (middle, n=6-8 mice per group) total white blood cell counts (WBC) and from KEP and WT mice (n=6 per group). Mann-Whitney *U*-test, $p < 0.05$ considered significant. Box and whisker plot: boxes represent median and interquartile range; whiskers represent full range.

(B) Representative flow cytometry plots from BM (left) and spleen (right) of myeloid-committed progenitors including MEP, CMP, GMP, MDP/cMoP and CDP.

(C) Quantification of absolute counts per spleen of myeloid-committed progenitors from WT (n=3) and KEP (n=4) mice. All comparisons not significant, Mann-Whitney test with multiple comparison correction and mean indicated.

Supplemental Figure 4

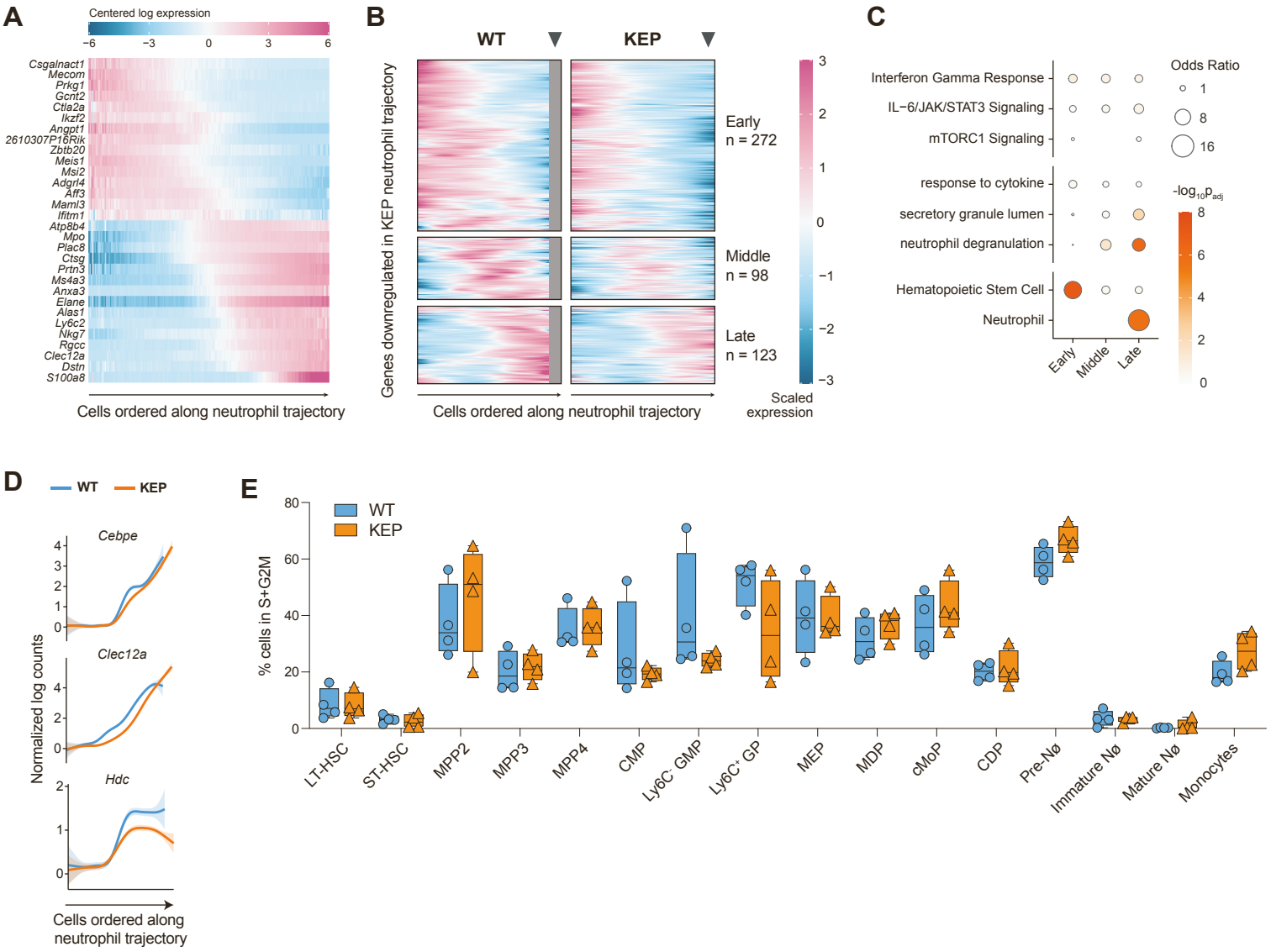

Figure S4. Downregulated gene sets in HSPC from mammary tumor-bearing mice.
Related to Figure 2

(A) Heatmap showing the mean-centered log expression of 15 genes showing the largest increase and decrease in expression along neutrophil pseudotime.

(B) Heatmap showing the scaled expression of genes downregulated in KEP cells along neutrophil pseudotime. Genes were grouped into three clusters based on the expression patterns.

(C) Enrichment of gene sets for groups of genes in B, using databases available through Enrichr[79]: GO: Biological Process, Reactome and Tabula muris.

(D) Example expression dynamics of selected downregulated genes along neutrophil pseudotime.

(E) Cell cycle analysis as determined by Ki-67 and DAPI staining from WT and KEP mice, n=4 mice per group. Box and whisker plots: boxes represent median and interquartile range; whiskers represent full range.

Supplemental Figure 5

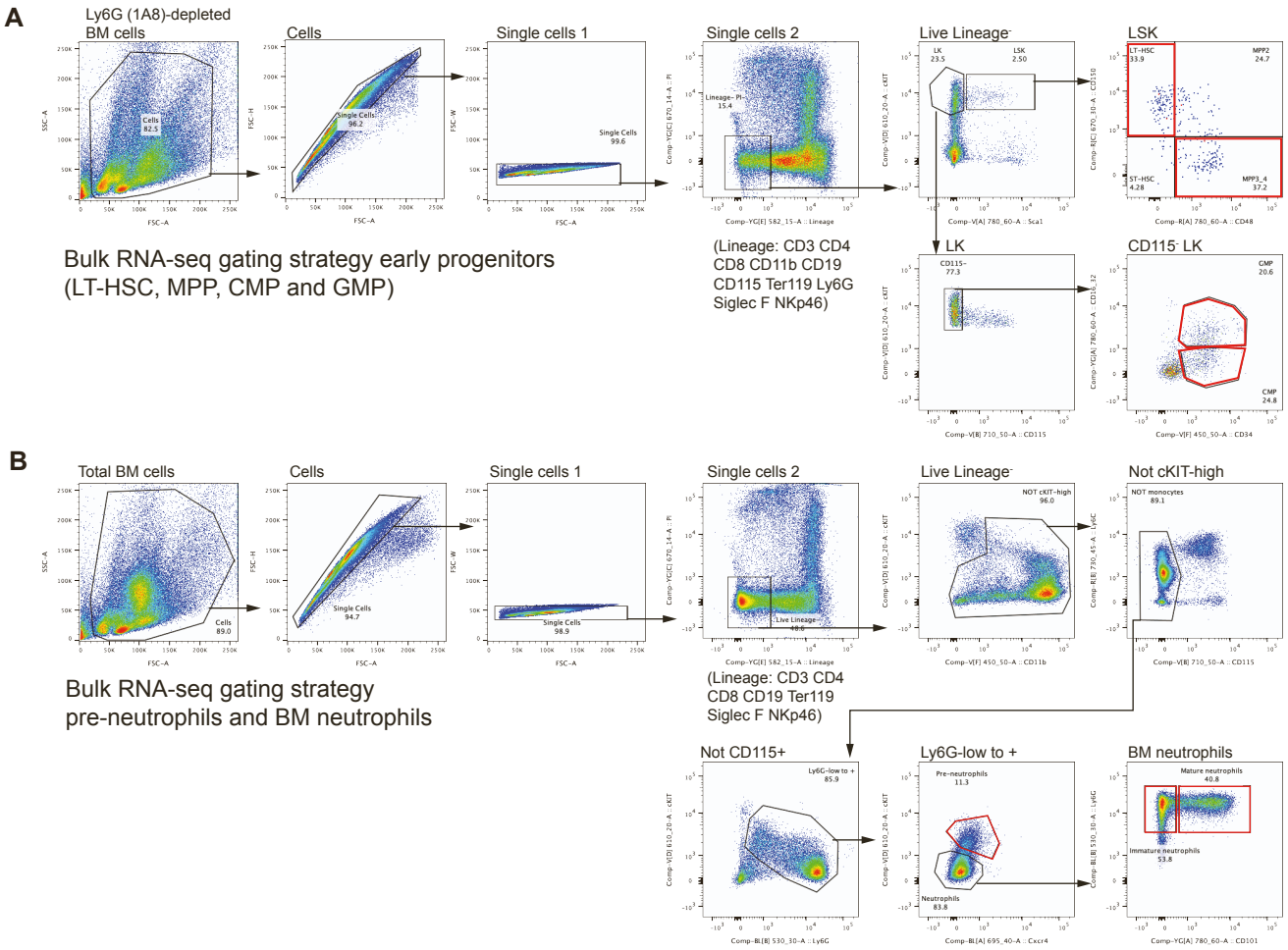

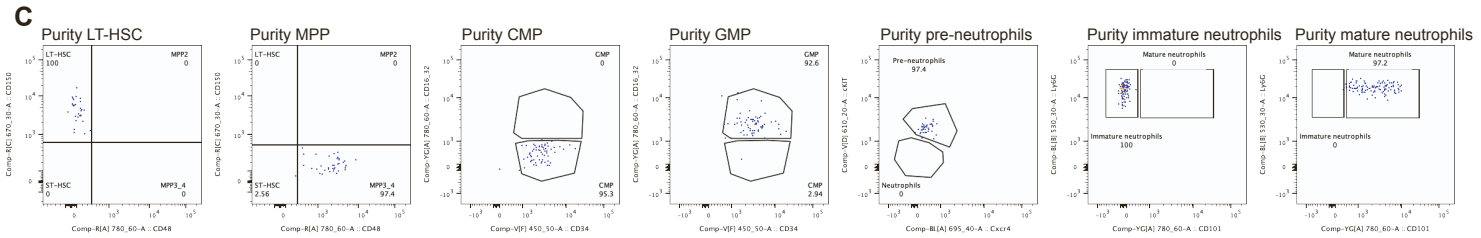

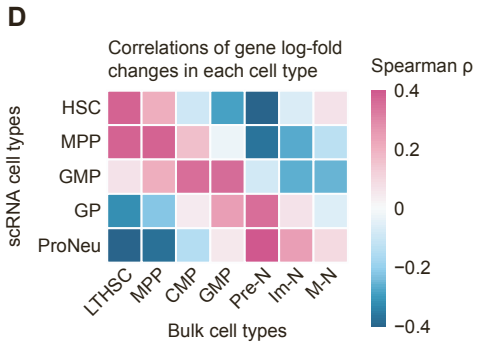

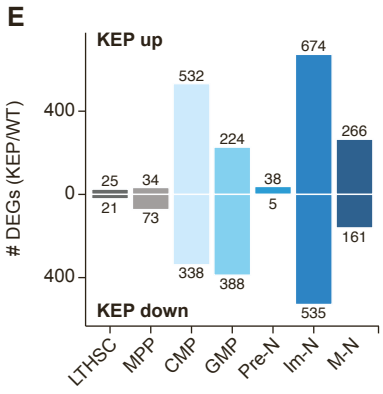

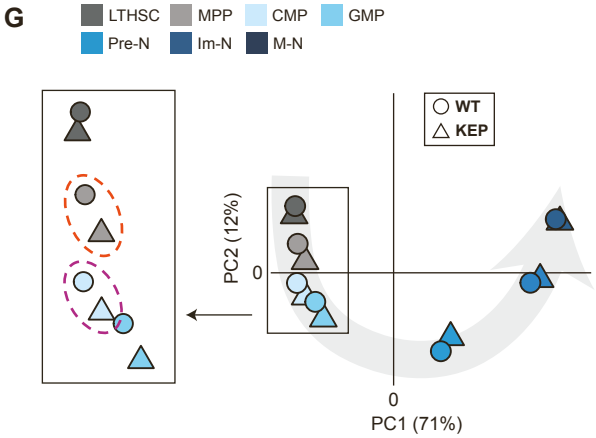

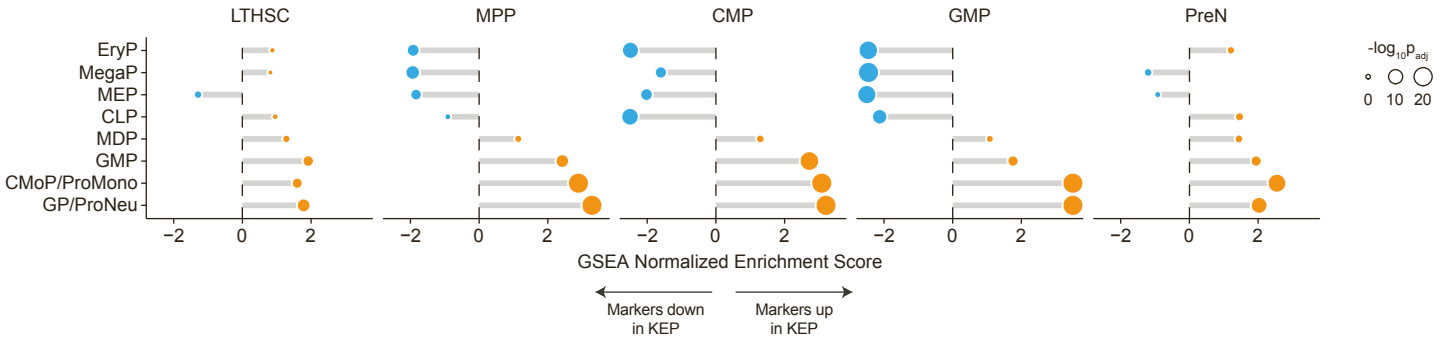

Figure S5. Bulk RNA-seq correlates with scRNA-seq

Related to Figure 3

(A and B) Gating strategies for sorting (A) early BM progenitors (LT-HSC, MPP, CMP, GMP) from neutrophil (1A8)-depleted BM and (B) committed BM neutrophils (pre-neutrophils, immature and mature neutrophils from total BM.

(C) Representative purity plots for the gating strategies reported in A and B.

(D) Spearman correlation between bulk RNA-seq sorted cell populations (columns) and scRNA-seq clustered populations (rows), using log fold changes of genes in each cell population compared to the average of other populations.

(E) Number of differentially expressed genes (FDR<0.05) in KEP compared to WT cell populations.

(F) GSEA using gene sets consisting of genes that show expression specific to different hematopoietic lineages, defined from our scRNA-seq data. GSEA was performed on genes ranked based on their bulk RNA-seq log fold changes in KEP vs WT comparison for each cell population.

(G) PCA was performed using normalized bulk RNA-seq expression for WT (circles) and KEP (triangles) cell populations. Shown are the first two PCs which recapitulate the neutrophil differentiation trajectory. The inset shows zoom-in onto progenitors which show accelerated differentiation phenotype.

Supplementary Figure 6

A

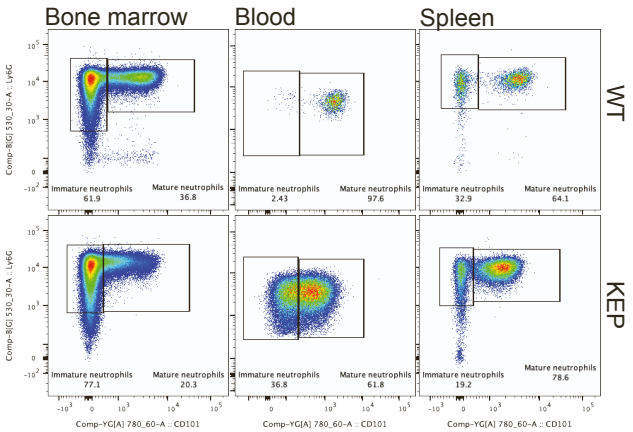

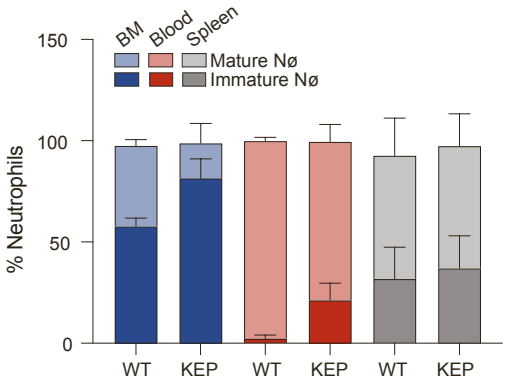

B

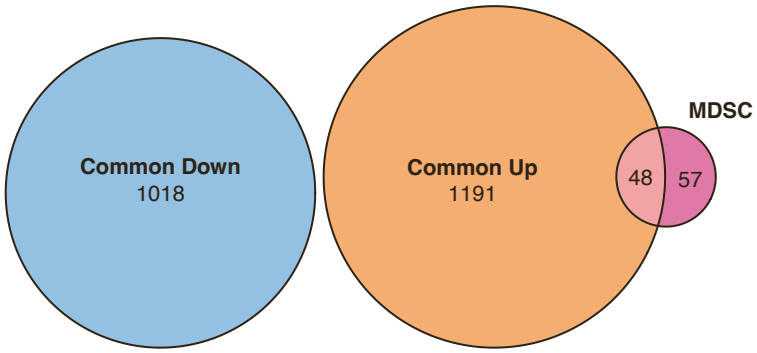

Figure S6. Neutrophils across tissues

Related to Figure 4

(A) Representative flow cytometry plots showing the relative proportion of immature ($Ly6G^+$ $CD101^-$) and mature ($Ly6G^+$ and $CD101^+$) neutrophils in BM, blood and spleen (left) and quantification (right).

(B) Venn diagram illustrating the common up and down regulated genes in neutrophils from tumor-bearing mice and the overlap between common upregulated genes and a previously defined immunosuppressive gene signature[28]. Fisher's exact test.

Supplemental Figure 7

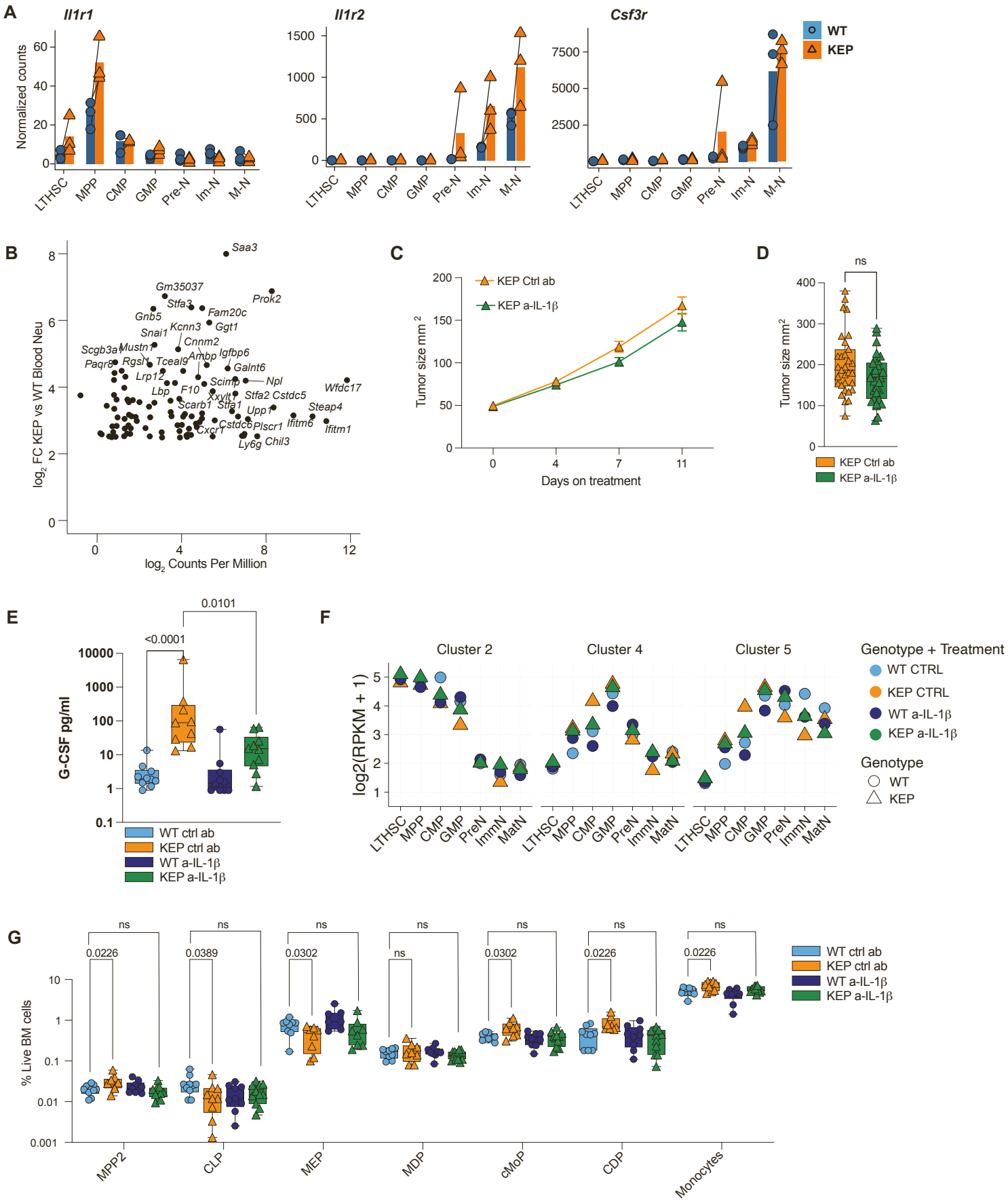

Figure S7. Treatment with anti-IL-1β normalizes hematopoiesis.

Related to Figure 5

(A) Bulk RNA-seq expression of *Il1r1, Il1r2* and *Csf3r* in HSPCs from WT (blue, n=3) and KEP (orange, n=3) mice.

(B) MA plot of top 100 genes by fold change upregulated in blood neutrophils from tumor-bearing KEP mice compared to blood neutrophils from tumor-free WT littermate controls (age matched).

(C) Average primary tumor growth curve ± SEM of KEP mice treated with anti-IL-1β (green) or isotype control (orange).

(D) End-stage primary tumor size (area) from isotype control (orange) or anti-IL-1β (green) treated KEP mice (n=31 mice per group).

(E) Serum concentration of G-CSF in mice WT mice treated with isotype control (light blue, n=10) or anti-IL-1β (dark blue, n=10) and KEP mice treated with isotype control (orange, n=9) or anti-IL-1β (green, n=10).

(F) Average normalized log accessibility for each of the three major clusters of differential chromatin accessibility identified in Figure 3 (clusters 2, 4, 5).

(G) Flow cytometry analysis of BM population frequencies from WT control (n=10, blue), KEP control (n=10, orange), WT anti-IL-1β (n=10, dark blue) and KEP anti-IL-1β (n=10, green) mice.

Statistics: Mann-Whitney *U*-test (D and E) or Mann-Whitney with Benjamini, Krieger and Yekutieli's multiple comparison correction (G), p- and q-values <0.05 considered significant. Data collected across 10 independent experiments. Box and whisker plots: boxes represent median and interquartile range; whiskers represent full range.